

1 **Spatial and temporal uncertainty of crop yield aggregations**

2 Vera Porwollik^a, Christoph Müller^a, Joshua Elliott^{b,c}, James Chrystanthacopoulos^c, Toshichika Iizumi^d,
3 Deepak K. Ray^e, Alex C. Ruane^{c,f}, Almut Arneith^g, Juraj Balkovič^{h,i}, Philippe Ciais^j, Delphine Deryng^{b,c},
4 Christian Folberth^{h,k}, Roberto C. Izaurralde^{l,m}, Curtis D. Jones^l, Nikolay Khabarov^h, Peter J. Lawrenceⁿ,
5 Wenfeng Liu^o, Thomas A.M. Pugh^{g,p}, Ashwan Reddy^l, Gen Sakurai^d, Erwin Schmid^q, Xuhui Wang^{i,r},
6 Allard de Wit^s, Xiuchen Wu^j

7 **Corresponding author**

8 Tel.: +49 331 288 20824; email: vera.porwollik@pik-potsdam.de; Potsdam Institute for Climate
9 Impact Research, Telegraphenberg 31, 14473 Potsdam, Germany

10 **Highlights**

- 11 • We aggregate 14 simulated gridded crop yields with four harvested areas data sets
12 • Uncertainties in multi-annual means and temporal patterns are quantified
13 • Aggregation uncertainties can be substantial but are often small
14 • Aggregation uncertainty should be considered in model evaluation and impact studies

15 **Keywords**

16 Aggregation uncertainty, global crop model, crop yields, gridded data, harvested area

^a Potsdam Institute for Climate Impact Research, Research Domain II Climate Impacts & Vulnerabilities, 14473 Potsdam, Germany

^b Columbia University Center for Climate Systems Research, NASA Goddard Institute for Space Studies, New York, NY 10025, USA

^c University of Chicago and ANL Computation Institute, Chicago, IL 60637, USA

^d National Agriculture and Research Organization, Institute for Agro-Environmental Sciences, Tsukuba, 305-8604, Japan

^e University of Minnesota, Institute on the Environment, Saint Paul, MN 55108, USA

^f NASA Goddard Institute for Space Studies, New York, NY 10025, USA

^g Karlsruhe Institute of Technology, IMK-IFU, 82467 Garmisch-Partenkirchen, Germany

^h International Institute for Applied Systems Analysis, Ecosystem Services and Management Program, 2361 Laxenburg, Austria

ⁱ Comenius University in Bratislava, Department of Soil Science, 842 15 Bratislava, Slovak Republic

^j Laboratoire des Sciences du Climat et de l'Environnement, CEA CNRS UVSQ, Orme des Merisiers, 91191 Gif-sur-Yvette, France

^k Ludwig Maximilian University, Department of Geography, 80333 Munich, Germany

^l University of Maryland, Department of Geographical Sciences, College Park, MD 20742, USA

^m Texas A&M University, Texas AgriLife Research and Extension, Temple, TX 76502, USA

ⁿ National Center for Atmospheric Research, Earth System Laboratory, Boulder, CO 80307, USA

^o Swiss Federal Institute of Aquatic Science and Technology, Eawag, CH-8600 Duebendorf, Switzerland

^p University of Birmingham, School of Geography, Earth & Environmental Science and Birmingham Institute of Forest Research, B15 2TT Birmingham, United Kingdom

^q University of Natural Resources and Life Sciences, Institute for Sustainable Economic Development, 1180 Vienna, Austria

^r Peking University, Sino-French Institute of Earth System Sciences, 100871 Beijing, China

^s Alterra Wageningen University and Research Centre, Earth Observation and Environmental Informatics, 6708PB Wageningen, Netherlands

17 **Abstract**

18 The aggregation of simulated gridded crop yields to national or regional scale requires information
19 on temporal and spatial patterns of crop-specific harvested areas. This analysis estimates the
20 uncertainty of simulated gridded yield time series related to the aggregation with four different
21 harvested area data sets. We compare aggregated yield time series from the Global Gridded Crop
22 Model Intercomparison project for four crop types from 14 models at global, national, and regional
23 scale to determine aggregation-driven differences in mean yields and temporal patterns as measures
24 of uncertainty.

25 The quantity and spatial patterns of harvested areas differ for individual crops among the four data
26 sets applied for the aggregation. Also simulated spatial yield patterns differ among the 14 models.
27 These differences in harvested areas and simulated yield patterns lead to differences in aggregated
28 productivity estimates, both in mean yield and in the temporal dynamics.

29 Among the four investigated crops, wheat yield (17% relative difference) is most affected by the
30 uncertainty introduced by the aggregation at the global scale. The correlation of temporal patterns of
31 global aggregated yield time series can be as low as for soybean ($r=0.28$).

32 For the majority of countries, mean relative differences of nationally aggregated yields account for
33 10% or less. The spatial and temporal difference can be substantial higher for individual countries. Of
34 the top-10 crop producers, aggregated national multi-annual mean relative difference of yields can
35 be up to 67% (maize, South Africa), 43% (wheat, Pakistan), 51% (rice, Japan), and 427% (soybean,
36 Bolivia). Correlations of differently aggregated yield time series can be as low as $r=0.56$ (maize, India),
37 $r=0.05$ (wheat, Russia), $r=0.13$ (rice, Vietnam), and $r=-0.01$ (soybean, Uruguay). The aggregation to
38 sub-national scale in comparison to country scale shows that spatial uncertainties can cancel out in
39 countries with large harvested areas per crop type. We conclude that the aggregation uncertainty
40 can be substantial for crop productivity and production estimations in the context of food security,
41 impact assessment, and model evaluation exercises.

42 **1. Introduction**

43 Crop models are increasingly applied at the global scale to study how agricultural yields and total
44 production over regions might be affected by global phenomena such as market dynamics and
45 climate change. Simulations of crop productivity (yield) at different spatial and temporal scales have
46 been used for example in the context of food security, land use, and climate change (Asseng et al.,
47 2015; Challinor et al., 2014; Mueller et al., 2012; Nelson et al., 2014a,b). Uncertainties associated
48 with crop model projections have been widely recognized and discussed, including those attributed
49 to input uncertainty (Roux et al., 2014), as to differences in climate forcing data (Rosenzweig et al.,
50 2014), model structure and parameterization (Rötter et al., 2012), and assumptions on the
51 effectiveness of CO₂-fertilization on crop yields (Deryng et al., 2014). The uncertainty in cropland
52 extent and its implications for land use modeling have been addressed before by Eitelberg et al.
53 (2015), Fritz et al. (2015), and See et al. (2015).

54 Gridded cropping system data sets on the spatial distribution of crops at the global scale have been
55 reported by Leff et al. (2004), and more recently by Iizumi et al. (2014), and Ray et al. (2012)
56 including distinct data on crop-specific harvested area. Anderson et al. (2015) directly compared four
57 gridded cropping system data sets as MIRCA2000 (Portmann et al., 2010), SPAM2000 (You et al.,
58 2014), GAEZ (Fischer et al., 2012), and M3 (Monfreda et al., 2008). They conclude that the data sets'
59 differences in harvested area and yield could be attributed mainly to the input data used and the
60 downscaling method applied, and report that the disagreement between data sets was largest in
61 areas with minimal harvested area. Different schemes for the interpolation of site-specific yields for
62 the aggregation to agro-climatic zones have been discussed by van Wart et al. (2013) within the
63 context of yield gap and production analysis.

64 Global gridded crop model (GGCM) results e.g. yield (t/ha) are typically reported in a standardized
65 half degree grid format. This output is aggregated at annual time steps to different spatial scales
66 within the context of model skill assessment, impact studies, or as input variable to land use models.
67 It is used for example when comparing different countries or evaluating modeled yields against

68 agricultural statistics that are only available at the aggregated scale of administrative units. For this
69 kind of aggregation, data sets on spatial patterns of crop-specific harvested area are applied, which
70 are typically derived from data on cropland extent, national and sub-national census data, and
71 allocation rules. To date, little attention has been paid to the uncertainty of aggregation of gridded
72 crop model simulations induced by the choice of crop-specific harvested area data set. Thus the
73 objective of this study is to assess this aggregation uncertainty at different spatial scales. We use the
74 term “crop mask” in the following as a short version of “gridded crop-specific harvested area data
75 set”. The uncertainty in simulated yields related to aggregation masks is determined by two factors:
76 a) the differences in quantity and spatial patterns of crop-specific harvested area data sets, and b)
77 the spatial and quantitative heterogeneity of simulated crop yields, which is specific to individual
78 GGCMs.

79 **2. Material and methods**

80 **2.1 Model input data and crop yield simulations**

81 In the Global Gridded Crop Model Intercomparison (GGCMI) project Phase 1
82 (<http://www.agmip.org/ag-grid/ggcmi/>) of the Agricultural Model Intercomparison and Improvement
83 Project (AgMIP) (Rosenzweig et al., 2013) 14 modeling groups performed historical global crop
84 growth simulations according to the modeling protocol of Elliott et al. (2015). Crop growth has been
85 simulated using the bias-corrected historical weather input data sets AgMERRA (Ruane et al., 2015)
86 and the atmospheric CO₂-data based on the Mauna Loa Observatory time series (Thoning et al.,
87 1989). AgMERRA provides daily data for the time period 1980-2010 and had been aggregated from
88 the original resolution of 0.25° to 0.5° before being supplied to modelers. The Mauna Loa
89 Observatory time series reports observed annual and monthly values of the atmospheric CO₂-mixing
90 ratio, so that models simulated crop growth with a CO₂-mixing ratio of 339-390ppmv (here stating
91 annual averages 1980-2010).

92 Four crop types were simulated by the modeling teams: maize (*Zea mays* L.), wheat (*Triticum*
93 *aestivum* L.), rice (*Oryza sativa* L.), and soybean (*Glycine max* (L.) Merr.) These crops had been

94 categorized in the GGCM project as Priority 1 crops, because of their importance as agricultural
 95 commodity in terms of their global harvested area covered, production amount, level of trade, and
 96 direct or indirect contribution to human diet.

97 The participating models cover a broad range of model types and of implemented processes. Their
 98 basic characteristics and key literature references are listed in Table 1 (more details in *SI Appendix*
 99 Tables A.1-5).

100 **Table 1:** Participating models in the study

Crop model	Model type	Key literature
CGMS-WOFOST	Empirical/process hybrid	de Wit van Diepen (2008)
CLM-Crop	Dynamic Global Vegetation Model	Drewniak et al. (2013)
EPIC-BOKU	Site-based process model (based on EPIC)	EPIC v0810 - Izaurre et al. (2006), Williams (1995)
EPIC-IIASA	Site-based process model (based on EPIC)	Izaurre et al. (2006), Williams (1995)
EPIC-TAMU	Site-based process model (based on EPIC)	EPIC v1102- Izaurre et al. (2012)
GEPIC	Site-based process model (based on EPIC)	EPIC v0810 - Liu et al. (2007), Williams (1995)
LPJ-GUESS	Dynamic Global Vegetation Model	Lindeskog et al. (2013), Smith et al. (2001)
LPJmL	Dynamic Global Vegetation Model	Waha et al. (2012), Bondeau et al. (2007)
ORCHIDEE-crop	Dynamic Global Vegetation Model	Wu et al. (2015)
pAPSIM	Site-based process model	APSIM v7.5 - Elliott et al. (2014), Keating et al. (2003)
pDSSAT	Site-based process model	pDSSAT v1.0 - Elliott et al. (2014); DSSAT v4.5 - Jones et al. (2003)
PEGASUS	Empirical/process hybrid	v1.1- Deryng et al. (2014), v1.0 - Deryng et al. (2011)
PEPIC	Site-based process model (based on EPIC)	EPIC v0810- Liu et al. (2016), Williams (1995)
PRYSBI2	Empirical/process hybrid	Sakurai et al. (2014)

101 For the crop growth simulations initial conditions of soil water, minerals, crop residues, and soil
 102 organic matter were derived by applying different soil input data and spin-up runs individual to each
 103 of the modeling groups (*SI Appendix* Table A.3). Modelers were asked to model all crops wherever a
 104 given crop can grow and at least on all current agricultural land. The GGCM project distinguishes
 105 three levels of model harmonization with respect to agricultural management. We here used the
 106 simulations of the “default” model configuration if available, where every modeling team used their
 107 own assumptions on agricultural management (varieties, growing season, fertilizer etc.). The EPIC-
 108 TAMU model was run at the global scale for the first time and ORCHIDEE-crop never globally
 109 simulated soybean before and thus could not provide a “default” simulation. These teams used the
 110 global input data on sowing and maturity dates, and fertilizer data provided within the context of the

111 GGCM project for a rather harmonized simulation, so that for this study their “fullharm” model
 112 configuration was used. The modeling teams reported two separate yield time series per
 113 configuration type - one assuming rainfed and the other fully irrigated production conditions
 114 everywhere. The irrigated crop growth simulations were run assuming unlimited water supply
 115 without conveyance or application losses.

116 As a second step we used crop yield simulations of seven models for the same four crop types of the
 117 Intersectoral Impact Model Intercomparison (ISI-MIP) and The Agricultural Model Intercomparison
 118 and Improvement Project (AgMIP) fast track (Rosenzweig et al., 2014) obtained from the open-access
 119 impact model data archive of ISI-MIP (<http://esg.pik-potsdam.de/>). These models were driven by
 120 output data from five climate models here for the RCP 8.5 pathway, including the suite of processes
 121 related to “CO₂- fertilization” for the future period 2070-2099 (modified carboxylation, and in some
 122 models reduced stomatal closure). Note that the seven models: EPIC-BOKU (in ISI-MIP/AgMIP fast
 123 track refer to the name “EPIC”), GEPIC, GAEZ-IMAGE, LPJ-GUESS, LPJmL, pDSSAT, PEGASUS which
 124 took part in the ISI-MIP/AgMIP fast track, also participated in this GGCM phase 1 study (model
 125 details are listed in *SI Appendix* Tables A.1-5), except the GAEZ-IMAGE model.

126 2.2 Crop masks

127 Four crop masks were used to aggregate simulated gridded yields: MIRCA2000 (Portmann et al.,
 128 2010), lizumi (lizumi et al., 2014), Ray (Ray et al., 2012), and SPAM2005 (You et al., 2014). Data
 129 sources and main characteristics of the original cropping system data sets were summarized in Table
 130 2.

131 **Table 2**

132 Major features of the four harvested area data sets applied for aggregation

Feature	MIRCA2000	lizumi	SPAM2005	Ray
Harvested area based on	Monfreda et al. (2008) - with modifications, circa 2000	Monfreda et al. (2008) - circa 2000	FAOSTAT, AGROMAPS and own sub-national data collection, circa 2005	Sub-national data collection (70% to 90%) 1961-2008
National areas	ESRI 2004	Dominant country code per 0.5° grid cell	Same national total areas as in MIRCA2000 (You et al., 2014)	As in Ramankutty et al. (2008)

N° of crops covered	26 crop classes	Maize, soybean, wheat, and rice	20 major crops	Maize, soybean, wheat, and rice
Original resolution	5 arc minute, 0.083° (~10km)	67.5 arc minute, 1.125° (~120km)	5 arc minute, 0.083° (~10km)	5 arc minute, 0.083° (~10km)
Irrigation data based on	Global Map of Irrigation Areas v.4 (Siebert et al., 2007, 2005), AQUASTAT national data	None	Global Map of Irrigation Areas v.5 (Siebert et al., 2007, 2005)	None
Cropland extent based on	Ramankutty et al. (2008)	Ramankutty et al. (2008)	Ramankutty et al. (2008)	Ramankutty et al. (2008)
Data inclusion method	Collection of statistical data and literature	Yield estimation model	Cross entropy approach with spatial allocation model optimization	Administrative bottom-up statistical data inclusion

133

134 All four data products were based on the cropland extent (ha) per grid cell by Ramankutty et al.
135 (2008), who merged sub-national and national inventory data with two global satellite based land
136 cover products. MIRCA2000 and IZUMI rely on the harvested area data of Monfreda et al. (2008) who
137 used about 50% of sub-national and also FAO-based national data averaged over the time period
138 1997-2003. SPAM2005 is the update of the former SPAM2000 data set, wherein the share of sub-
139 national data collection for harvested area was about 50% and Ray's share of that was 70-90% - the
140 rest of both had been complemented with FAO national data as well. MIRCA2000, IZUMI, and
141 SPAM2005 report static harvested area data per grid cell (circa 2000 or 2005) whereas Ray provides a
142 dynamic annual time-series (1961-2008). MIRCA2000 and SPAM2005 independently report the
143 spatial distribution of irrigated and rainfed harvested areas (ha) per crop type, which is an important
144 feature for crop modeling and aggregation but are based on different baseline years (2000 vs. 2005).
145 The IZUMI and Ray data sets do not further distinguish harvested areas into irrigated and rainfed
146 fractions. The four data sets display differences in spatial patterns of harvested area as highlighted by
147 Fig. 1 for maize (for the other crops see *SI Appendix*, Fig. B.1-4)
148 {Placeholder Figure 1}

149 2.3 Pre-processing the crop masks

150 The IZUMI data set, originally reported at a spatial resolution of 1.125°, was interpolated to 0.5°.
151 MIRCA2000, SPAM2005, and Ray originally provided data at 5 arc minutes resolutions, which we
152 aggregated to 0.5°. The original information on cropland extent and harvested area around the year

153 2000 from MIRCA2000, IZUMI, and SPAM2005 data sets, were kept constant and used to aggregate
 154 the simulated yields for the time period 1980-2010. The original Ray data set covered all simulated
 155 years up to 2008 and the aggregated yield time series used for this analysis thus spanned only the
 156 years 1980-2008. All aggregations with SPAM2005 and MIRCA2000 were performed with their own
 157 shares of rainfed and irrigated areas. In the case of the Ray and IZUMI data sets, their harvested area
 158 per grid cell were split into irrigated and rainfed fractions using MIRCA2000's relative shares for a
 159 given crop in each 0.5° grid cell. Grid cells, for which MIRCA2000 specifies no harvested area for the
 160 crop of interest, were assumed to be without irrigation if they contained crops in the original Ray or
 161 IZUMI data sets.

162 **2.4 Aggregating gridded yield data**

163 The GGCMs simulations provided crop yield data in tons of dry matter per hectare (t/ha) for four
 164 crop types under fully rainfed and fully irrigated conditions in annual time steps within the time
 165 period 1980-2010. These grid cell-specific yield estimates have been aggregated to time series at
 166 three spatial scales: global, country, and food production unit (FPU, major river basins crossed with
 167 countries) (Cai and Rosegrant, 2002) using the four crop masks as weights in the averaging (equation
 168 1):

$$yield_{aggregated} = \frac{\sum_{i=1}^n yield_{i_i} * area_{irrigated_i} + \sum_{i=1}^n yield_{i_r} * area_{rainfed_i}}{\sum_{i=1}^n (area_{irrigated_i} + area_{rainfed_i})}$$

169 i: any grid cell in the aggregation unit

170 n: number of grid cells in the aggregation unit

171 $yield_{i_i}$: simulated yield (t/ha) under full irrigated conditions in grid cell i

172 $yield_{i_r}$: simulated yield (t/ha) under rainfed conditions in grid cell i

173 $area_{irrigated_i}$: irrigated harvested area (ha) in grid cell i

174 $area_{rainfed_i}$: rainfed harvested area (ha) in grid cell i

175 To derive the productivity (t/ha) per year and aggregation unit, each rainfed yield, simulated by the
 176 models in a corresponding grid cell, is multiplied with the rainfed harvested area. The same

177 procedure was carried out for the irrigated yields. Then the sum of all rainfed and irrigated
178 production is divided by the total sum of harvested area reported by the individual data sets of that
179 spatial aggregation unit, resulting in the aggregated mean yield (t/ha) per year and aggregation unit.
180 Grid cells were assigned to countries according to the boundary information of Global Administrative
181 Areas (GADM-0, <http://gadm.org/>), assigning grid cells to the country that has the largest area share
182 in that grid cell. Here we used information on crop specific harvested areas, which can be larger than
183 the physical cropland extent in multiple cropping systems with several harvests per year, which was
184 accounted for in the harvested area data sets. The GGCMs simulated only a single growing period per
185 grid cell, which we assume to be representative for the different growing periods due to current
186 state of implementation of cropping management systems in the models.

187 For an assessment of aggregation uncertainties in projections of future changes in crop productivity,
188 simulated gridded future yields of the ISI-MIP/AgMIP fast track are aggregated to country scale by
189 three different time slices (1961, 1984 and 2008) of the Ray data set.

190 In order to quantify the differences between the different crop mask aggregations, we display
191 absolute (t/ha) and relative (%) differences between yield aggregated with each of the four masks:
192 MIRCA2000 (further abbreviated as MIRCA), Ray, IZUMI, and SPAM2005 (in the following abbreviated
193 as SPAM) for selected regions/countries as well as by computing the yield time series differences
194 over time. The correlation coefficients between the differently aggregated time series were used to
195 describe how yield aggregates of individual years are affected by the different crop masks and how
196 this affects variability over time. If all years were affected equally, aggregated yield time series differ
197 in their mean but are highly correlated. Data analysis was conducted in R (R Development Core
198 Team, 2014), using the standard Pearson correlation (Becker et al., 1988).

199 **3. Results**

200 The different crop masks lead to different yield estimates for individual years at all spatial scales
201 (global, national, and FPU). The mean relative differences among aggregated global yields reach up to
202 6 % for maize, 17 % for wheat, 14 % for rice, and 10% for soybean across the different crop models

203 (further details at bottom of the Tables 3-6). The ranges depended on the heterogeneity of the
204 simulated spatial yield patterns by the GGCMs and how strongly opposing deviations in different
205 regions compensate each other. The aggregation with different crop masks also affects the simulated
206 temporal dynamics, with minimum correlation coefficients between the global aggregated yield time
207 series of $r=0.77$ for maize, $r=0.85$ for wheat, $r=0.64$ for rice, and $r=0.28$ for soybean (Tables 3-6).

208 Across 208 countries, 14 GGCMs, and 31 years, aggregation induced differences between nationally
209 aggregated yield estimates for the four crop types can be very large (>10 DM t /ha), but the majority
210 is below 10% of relative difference (<0.3 DM t/ha in absolute terms). The aggregations with Ray show
211 least differences to aggregations with MIRCA, whereas SPAM-based aggregations show strongest
212 differences to MIRCA, IZUMI, and Ray-based aggregations (Fig. 2). Largest relative differences in yield
213 sets can be found for soybean especially in comparison of SPAM to each of the other three
214 aggregated sets. Aggregated maize yield are least affected by the aggregation uncertainty.

215 {Placeholder figure 2}

216 When accounting for differences in total crop area, e.g. when looking at differences in production (t)
217 rather than in productivity (t/ha), the relative differences between country scale aggregations are
218 even stronger (Fig. C in the *SI Appendix*). This is caused by differences in quantity and spatial pattern
219 of the harvested area data set applied for the aggregations. At the national level, the crop cover
220 mask can be of greater importance. In the Tables 3-6, the effects of different aggregations on country
221 scale are displayed for the top-ten producer (for all countries and the four crops Tables D.1-4 in the *SI*
222 *Appendix*). Differences over the 31 years are shown as the percentage minimum and maximum mean
223 relative difference between the aggregations with Ray, IZUMI, SPAM, and MIRCA-based aggregation.
224 Differences in temporal dynamics induced by the different crop masks applied for the aggregation
225 are shown by the minimum correlation coefficient (r) between aggregated national time series (one
226 per GGCM). Countries were ranked by their share on global production as averaged over the years
227 2009-2013 (FAO, 2014).

228 **Table 3:** Lowest and highest values of mean relative difference (%) and the lowest correlation
 229 coefficient (r) between the aggregated maize yield time series (t/ha) calculated from the 14 models,
 230 during the AgMERRA time period, aggregated for the top-10 producer countries with one harvested
 231 area data set in relation to the aggregation with each of the other three masks (see more detailed
 232 results for all countries in *SI Appendix* Table D.1).

maize top-10 producer countries	lowest value of relative difference (%)	masks lowest value of relative difference	highest value of relative difference (%)	masks highest value of relative difference	minimum correlation (r)	masks minimum correlation	Share on global production (%)
USA	-3	SPAM-MIRCA	2	Ray-MIRCA	0.98	Ray-lizumi	35.74
China	-11	SPAM-MIRCA	8	Ray-SPAM	0.94	Ray-SPAM	21.54
Brazil	-9	SPAM-MIRCA	7	Ray-SPAM	0.95	Ray-lizumi	7.04
Argentina	-7	lizumi-MIRCA	10	Ray-lizumi	0.93	Ray-lizumi	2.54
Mexico	-14	SPAM-MIRCA	17	Ray-SPAM	0.71	Ray-SPAM	2.38
India	-21	SPAM-MIRCA	38	Ray-SPAM	0.56	MIRCA-Ray	2.38
Ukraine	-11	lizumi-MIRCA	20	Ray-SPAM	0.96	lizumi-SPAM	2.18
Indonesia	-8	lizumi-MIRCA	6	Ray-MIRCA	0.85	lizumi-SPAM	2.06
France	-20	lizumi-SPAM	28	SPAM-MIRCA	0.95	MIRCA-lizumi	1.70
South Africa	-37	SPAM-MIRCA	67	lizumi-SPAM	0.75	MIRCA-SPAM	1.34
global	-5	Ray-lizumi	5	lizumi-MIRCA	0.77	MIRCA-Ray	100

233
 234 Of the top-10 maize producers (United States, China, Brazil, Argentina, Mexico, India, Ukraine,
 235 Indonesia, France, and South Africa) - South Africa, India, and France show stronger sensitivity to the
 236 choice of the aggregation mask, while the USA (*SI Appendix* Fig. F.3) is less sensitive to the choice of
 237 crop mask (for all countries see *SI Appendix* Table D.1). Of the top-10 maize producers, yield
 238 simulations can be strongly affected by the national aggregation mask by up to 67% (South Africa),
 239 38% (India) or 28% (France, Fig. 3). Individual years can be affected more strongly, so that the
 240 correlation between the MIRCA-based aggregated time series and the ones obtained with the Ray
 241 mask can be low, as in India ($r=0.56$), while the correlation is not necessarily low if there are stronger
 242 differences in mean yields (e.g. France with minimum $r=0.95$).

243 {Placeholder figure 3}

244 From the top-10 wheat producer countries (Table 4) Canada with -28-41% has the largest span of
 245 relative yield difference as well as a low correlation coefficient of $r=0.41$ (lizumi-SPAM). For Pakistan,
 246 differences in mean yield of up to 43% can be observed for the MIRCA-based aggregation compared
 247 to the one with lizumi. Only the mean relative difference between aggregated yield sets for Russia,

248 United States, France, and Germany are about 15% or less. For the case of wheat productivity in
 249 Russia low differences in yields are shown but the correlation coefficient reaches as low values as
 250 $r=0.05$ displaying the larger deviations of temporal patterns in aggregated yield sets (MIRCA-SPAM).

251 **Table 4:** Lowest and highest values of mean relative difference (%) and the lowest correlation
 252 coefficient (r) between the aggregated wheat yield time series (t/ha) calculated from the 14 models,
 253 during the AgMERRA time period, aggregated for the top-10 producer countries with one harvested
 254 area data set in relation to the aggregation with each of the other three masks (see more detailed
 255 results for all countries in (SI Appendix Table D.2).

wheat top-10 producer countries	lowest value of relative difference (%)	masks lowest value of relative difference	highest value of relative difference (%)	masks highest value of relative difference	minimum correlation (r)	masks minimum correlation	Share on global production (%)
China	-19	SPAM-MIRCA	19	lizumi-SPAM	0.82	SPAM-MIRCA	17.26
India	-16	SPAM-MIRCA	33	lizumi-SPAM	0.89	lizumi-SPAM	12.77
USA	-8	lizumi-MIRCA	7	Ray-lizumi	0.77	lizumi-SPAM	8.61
Russia	-6	lizumi-SPAM	6	lizumi-SPAM	0.05	SPAM-MIRCA	7.29
France	-5	lizumi-SPAM	6	Ray-lizumi	0.85	lizumi-MIRCA	5.60
Canada	-28	Ray-SPAM	41	SPAM-MIRCA	0.41	lizumi-SPAM	4.09
Australia	-21	lizumi-SPAM	16	SPAM-MIRCA	0.87	lizumi-SPAM	3.62
Pakistan	-19	SPAM-MIRCA	43	lizumi-MIRCA	0.79	SPAM-MIRCA	3.52
Germany	-4	lizumi-MIRCA	5	Ray-lizumi	0.94	MIRCA-Ray	3.50
Turkey	-17	lizumi-SPAM	15	SPAM-MIRCA	0.72	MIRCA-Ray	3.05
global	-17	SPAM-MIRCA	10	Ray-SPAM	0.85	MIRCA-Ray	100

256
 257 In the case of rice productivity (Table 5), relative differences between aggregations sets for Indonesia
 258 and Brazil are below 10%. Indonesia has fairly high correlation across all masks pairings but for Brazil
 259 the correlation between the MIRCA and Ray-based aggregations is as low as $r=0.32$. Rice yields for
 260 Vietnam, Philippines, Thailand, and Japan show very strong relative differences between aggregated
 261 yield sets. For rice in Vietnam also the temporal dynamics are affected by the choice of aggregation
 262 mask, reflected by a very low correlation coefficient of $r=0.13$ when comparing MIRCA- to SPAM-
 263 based aggregations.

264 **Table 5:** Lowest and highest values of mean relative difference (%) and the lowest correlation
 265 coefficient (r) between the aggregated rice yield time series (t/ha) calculated from 11 models, during
 266 the AgMERRA time period, aggregated for the top-10 producer countries with one harvested area

267 data set in relation to the aggregation with each of the other three masks (see more detailed results
 268 for all countries in *SI Appendix* Table D.3). Note that the models PEGASUS, PAPSIM, and EPIC-TAMU
 269 did not simulate rice.

rice top-10 producer countries	lowest value of relative difference (%)	masks lowest value of relative difference	highest value of relative difference (%)	masks highest value of relative difference	minimum correlation (r)	masks minimum correlation	Share on global production (%)
China	-25	lizumi-MIRCA	14	SPAM-MIRCA	0.71	MIRCA-Ray	27.99
India	-10	lizumi-SPAM	13	SPAM-MIRCA	0.88	MIRCA-Ray	20.97
Indonesia	-5	lizumi-MIRCA	4	Ray-SPAM	0.95	lizumi-SPAM	9.36
Bangladesh	-15	lizumi-SPAM	17	SPAM-MIRCA	0.97	MIRCA-SPAM	6.97
Vietnam	-33	lizumi-SPAM	42	SPAM-MIRCA	0.13	MIRCA-SPAM	5.81
Thailand	-29	lizumi-SPAM	35	SPAM-MIRCA	0.78	Ray-SPAM	4.97
Myanmar	-11	lizumi-SPAM	10	Ray-SPAM	0.92	MIRCA-SPAM	4.18
Philippines	-33	lizumi-SPAM	38	SPAM-MIRCA	0.77	Ray-SPAM	2.37
Brazil	-9	Ray-lizumi	8	lizumi-SPAM	0.32	MIRCA-Ray	1.69
Japan	-18	Ray-lizumi	51	lizumi-MIRCA	0.79	MIRCA-Ray	1.48
global	-14	lizumi-SPAM	11	SPAM-MIRCA	0.64	MIRCA-Ray	100

270

271 For soybean several countries show large relative differences attributed to the crop mask and the
 272 modelled yield patterns across the country. For soybean in Bolivia the relative difference between
 273 the Ray and the SPAM-based aggregation reach 427%, for Paraguay 82% between lizumi- and SPAM-
 274 based aggregations, followed by India with 48% relative yield difference between the Ray- and the
 275 SPAM-based aggregation. China and the United States show the lower sensitivity to the crop mask
 276 applied with ranging around 10% relative difference between the different aggregated yield sets.
 277 Although soybean yields of Brazil show relatively low sensitivity to the aggregation mask effects with
 278 23% as maximum relative difference, but the correlation coefficient of $r=0.07$ between the Ray- to
 279 SPAM-based aggregation is very low, displaying little agreement in temporal pattern between the
 280 time series. Temporal dynamics of soybean productivity in Uruguay, Canada, and India are greatly
 281 affected by the aggregation mask and can reach even negative correlation coefficients.

282 **Table 6:** Lowest and highest values of mean relative difference (%) and the lowest correlation
 283 coefficient (r) between the aggregated soybean yield time series (t/ha) calculated from 13 models,
 284 during the AgMERRA time period, aggregated for the top-10 producer countries with one harvested
 285 area data set in relation to the aggregation with each of the other three masks (see more detailed

286 results for all countries in *SI Appendix* Table D.4). Note that the model EPIC-TAMU did not simulate
 287 soybean.

soybean top-10 producer countries	lowest value of relative difference (%)	masks lowest value of relative difference	highest value of relative difference (%)	masks highest value of relative difference	minimum correlation (r)	masks minimum correlation	Share on global production (%)
USA	-4	Ray-SPAM	9	Ray-MIRCA	0.91	Ray-SPAM	34.52
Brazil	-8	lizumi-MIRCA	23	Ray-lizumi	0.07	Ray-SPAM	27.48
Argentina	-22	Ray-lizumi	25	lizumi-MIRCA	0.8	Ray-lizumi	17.51
China	-8	SPAM-MIRCA	14	lizumi-SPAM	0.83	Ray-SPAM	5.53
India	-13	SPAM-MIRCA	48	Ray-SPAM	-0.08	Ray-MIRCA	4.85
Paraguay	-41	SPAM-MIRCA	82	lizumi-SPAM	0.83	SPAM-MIRCA	2.61
Canada	-16	SPAM-MIRCA	20	Ray-SPAM	-0.23	SPAM-MIRCA	1.77
Uruguay	-16	Ray-SPAM	27	lizumi-SPAM	-0.01	Ray-SPAM	0.88
Ukraine	-9	SPAM-MIRCA	12	Ray-SPAM	0.82	Ray-SPAM	0.80
Bolivia	-68	SPAM-MIRCA	427	Ray-SPAM	0.45	Ray-SPAM	0.78
global	-6	SPAM-MIRCA	10	Ray-SPAM	0.28	Ray-SPAM	100

288 The differences due to aggregation can become exceptionally high in countries with pronounced
 289 differences in crop-specific harvested area information (*SI Appendix* Tables G.1-2) and where GGCMs
 290 simulate heterogeneous yield patterns, as reflecting strong gradients in climatic conditions or crop
 291 management practices. Strong yield gradients between grid cells within a country can also derive
 292 from model-specific calibration processes of e.g. simulated yields to observations of field
 293 experiments or country-specific reference data sets (*SI Appendix* Table A.5). The effect of calibration
 294 may even increase the aggregation uncertainty, which is exemplified by maize yield aggregations in
 295 Egypt (Fig. 4, *SI Appendix* Fig. E.1). In Egypt almost the entire maize production is irrigated. In Fig.4
 296 we show GGCM simulations of four different models. PEGASUS and PRYSBI2 simulate very
 297 heterogeneous yield patterns, whereas pDSSAT assumes more homogeneous and LPJmL simulates
 298 very homogeneous yield patterns, assuming national uniform crop production intensities.

299 {Placeholder figure 4}

300 In the case of model PRYSBI2, the only area with higher yields is around Port Said, for which only the
 301 lizumi crop mask reports some larger harvested area for maize (Fig. 4, *SI Appendix* G.1-2). PRYSBI2
 302 calibrates several parameters (more details in *SI Appendix* Table A.5) on grid cell level to best match
 303 the yields to the lizumi et al. (2014) yield reference data set in their “default” simulation.
 304 Consequently, aggregated PRYSBI2 yields are very low, except when aggregated with the lizumi crop
 305 mask, which results in an aggregated annual yield being up to 250% more productive compared to

306 the other aggregations. For the model PEGASUS, the productive harvested area is located along the
307 Mediterranean coastline. Calibration in PEGASUS consisted in tuning the radiation use efficiency
308 factor (β) to select a proper crop variety to best match the yield data of Monfreda et al. (2008)
309 according to the Willmott index of agreement. The aggregated national result for PEGASUS's yields
310 shows stronger differences for the SPAM aggregation, which reports less harvested maize areas
311 along the Mediterranean coast line. LPJmL calibrates its parameters: maximum leaf-area-index under
312 unstressed conditions, harvest index, and factor (α) for up-scaling leaf-level-photosynthesis to
313 stand level, at country scale, to best match the national yields reported by the FAO. LPJmL thus
314 simulated a very homogeneous yield pattern for irrigated maize in Egypt, as climatic conditions are
315 similarly very hot and dry - but irrigated across the area. The yields of pDSSAT are calibrated to field
316 experiment results. The maize yield pattern of pDSSAT for Egypt is less homogeneous than LPJmL as
317 it takes into account more spatial detail on fertilizer application and other management parameters.
318 Further analysis reveals that sub-regions of larger producing countries, as in individual FPU's of the
319 USA, show a mixed response. Major production areas of the USA along the Mississippi (*SI Appendix*
320 Fig. F.1), the Missouri, and the Ohio River catchments show very little sensitivity to the choice of the
321 crop mask. Other FPU's, such as the Colorado River catchment (*SI Appendix* Fig.F.2) or California,
322 show larger discrepancies between the aggregated yield sets. At the national scale, these regional
323 discrepancies do not show, as the national aggregated productivity is numerically dominated by the
324 major production areas, which show little sensitivity to the choice of the aggregation mask (*SI*
325 *Appendix* Fig. F.3)

326 Assuming static crop masks in the assessments of climate change impacts on agricultural productivity
327 can also strongly affect the projected impact on crop yields. We demonstrate this by aggregating the
328 climate change impact projections on yields of the ISI-MIP/AgMIP fast track (Rosenzweig et al., 2014)
329 with different time slices of the Ray crop mask (years: 1961, 1984, and 2008) as if the assessment had
330 been conducted in these years, assuming 'current' crop masks. We find strong effects on the
331 projected future yield changes in response to climate and elevated atmospheric CO₂ for individual

332 crops in some countries. Figure 5 shows the differences in projected relative yield changes
333 (percentage change of the period 2070-2099 relative to the 1980-2009 baseline) between the
334 country scale aggregation with the 1961 mask and the aggregation with the two other masks (1984
335 and 2008) for all seven models that contributed to the ISI-MIP/AgMIP fast track (Rosenzweig et al.,
336 2014). The differences in the five climate projections affect the heterogeneity of simulated yields and
337 thus the sensitivity of aggregated yield changes to the crop mask (bars and whiskers in Fig. 5). For
338 aggregated maize yield projections in India most models show a positive trend with time in projected
339 changes in yields. The projected difference in relative yield change simulated by EPIC-BOKU, GEPIC,
340 and pDSSAT models are considerably higher for the aggregation with Ray's harvested area time slice
341 of 2008 compared to the 1961 as the relative yield change of the aggregated yield with the 1984
342 mask compared to 1961er. For the case of wheat in Australia the projected yield changes agree quite
343 well, showing only slightly median differences between the time slices used for aggregation. Only the
344 EPIC-BOKU projections show a high variability and maximal difference of yield change of up to -10%
345 with the 2008er in comparison to the 1961 mask but only 4% difference for the 1984 in comparison
346 to the 1961 time slice. This is because the crop-specific harvested area regions in the former case
347 have changed a lot with significant expansion of harvested maize areas in southern India, whereas in
348 Australia the regions have remained roughly similar.

349 {Placeholder figure 5}

350 In the case of rice productivity in Brazil, aggregations with the crop mask of 2008 lead to higher
351 difference in yield change projections than the 1984 mask (except for GEPIC) compared to the
352 aggregation with the 1961 time slice. For soybean in Argentina the magnitude of differences in
353 projected yield change are less pronounced between the time-slices' aggregation used but are very
354 different among models as for pDSSAT, and LPJ-GUESS up to 20% but more than 40% for PEGASUS.
355 Differences in climate change impact projections for all other countries of the top-10 producer
356 countries are lower than for those countries displayed in Fig.5.

357 4. Discussion

358 We find that differences in crop masks affect not only the mean bias of aggregated yield time series
359 but also the temporal dynamics, resulting in low or even negative correlations between the
360 differently aggregated time series (Tables 3-6, and D.1-8 in the *SI Appendix*). This is of particular
361 concern, as model skill is often determined by comparing temporal dynamics rather than mean
362 yields. Large difference between aggregated yield time series occur, when areas suitable for crop
363 growth (determined by the individual model) are combined with a large harvested area reported by
364 one mask but rather little by another (Fig. 4, *SI Appendix*, Tables G.1-2). Developers of GGCMs need
365 to analyze the spatial variability of their simulations for plausibility. Models that tend to simulate
366 very heterogeneous patterns of crop yields due to calibration, flexible parameter specifications, and
367 assumptions on management practices (e.g. cultivar choice, fertilizer application, sowing dates) were
368 more sensitive to the choice of crop mask (*SI Appendix*, Table A.5). Further differences between the
369 aggregated productivity time series result from the fact, that spatial location of national borders of
370 the various original crop masks are different due to different data products included by the authors
371 (Table 2). When applying publicly available statistics for down-scaling data to a grid cell (as the
372 authors did to produce the harvested area data sets) its accuracy is also limited by the fact, that the
373 historical development of states cannot be well reflected in a timely manner. Also, we assume that
374 each grid cell always belongs to a single country, whereas often the simulated grid cell level results
375 would need to be attributed as fractions to multiple countries. However, since we treat this
376 consistently across the different crop mask data sets used, we consider the resulting error as not
377 relevant in the comparison of the different crop masks in the aggregation process.

378 The spatial patterns of crop-specific harvested areas as provided by the four data sets here used for
379 aggregation, and the information on where irrigation is applied for these crops is central to large-
380 scale crop modeling. The crop-modelling community requires more complex and updated data on
381 the spatial and temporal dynamics of agricultural production systems. The Ray data set is the only
382 crop mask that is dynamic in time and it also is typically the aggregation mask that shows the largest

383 differences in the temporal dynamics between the aggregated yield time series (low correlation
384 coefficients). We conclude that each of the four harvested area data sets has its unique features and
385 none can be identified as particularly superior by our study. For particular regions spatial
386 aggregations should be performed with alternative crop masks to assess the effects of aggregation
387 uncertainty and to avoid drawing erroneous conclusions on model skill or projected impacts.

388 Reporting productivity is what is typically done to communicate or analyze climate change impacts
389 on agriculture (e.g. Müller et al., 2015; Osborne et al., 2013; Wheeler and von Braun, 2013) or to
390 inform land use change models (Müller and Robertson, 2014; Nelson et al. 2014a,b; Schmitz et al.,
391 2014). With some exceptions, as e.g. GLOBIOM (Havlík et al., 2012, 2011) and MAgPIE (Dietrich et al.,
392 2014; Lotze-Campen et al., 2008), these models require information on changes in agricultural
393 productivity aggregated to their simulation units (because of their often coarser resolution, as e.g.
394 national or supra-national regions). General shifts of cropping areas towards higher productive areas
395 are very likely (Beddow and Pardey, 2015) as can be investigated by land use models, which project
396 changes in land use and production as socio-economic responses to changes in agricultural
397 productivity. Future land use uncertainty can also be addressed by aggregating simulated changes in
398 productivity with external land use scenarios as in Pugh et al. (2015) and remain a challenge for
399 further crop modeling studies.

400 **5. Conclusions**

401 This study shows quantitative differences between the aggregated gridded yield time series revealing
402 the uncertainty induced by the aggregation applying differing harvested area data sets. The effects of
403 aggregation uncertainty are the shift of the multi-annual mean national yield and an influence on the
404 variability over time, depending on the heterogeneity of simulated yield patterns by the models and
405 the differences between crop masks. This uncertainty is already significant in global aggregations of
406 grid cell scale yield simulations and can be very large for some aggregation-unit-crop-model-year
407 combinations. Aggregation uncertainty of gridded yields becomes even more important when taking

408 into account production instead of productivity. For projections of future agricultural production, this
409 aggregation uncertainty will likely be small compared to given uncertainties in future climate change,
410 adaptation options, and capacities. The potentially large differences between different aggregations
411 for individual countries or regions will have to be considered in future model evaluations and also in
412 future crop yield projections. This requires considerable investment for building a transparent
413 method for aggregation. The study also illustrates the need to transition from assuming static
414 harvested areas towards dynamic projections that account for spatial shifts in crop distribution and
415 production induced by changes in social and environmental conditions.

416 **Acknowledgement**

417 We acknowledge the support and data provision by the Agricultural Intercomparison and
418 Improvement Project (AgMIP), the Intersectoral Impact Model Intercomparison Project (ISIMIP), and
419 the contributing modelers. V.P. and C.M. acknowledge financial support from the MACMIT project
420 (01LN1317A) funded through the German Federal Ministry of Education and Research (BMBF). A.A.
421 and T.A.M.P. were supported by the European Commission's 7th Framework Programme
422 under Grant Agreement number 603542 (LUC4C) and by the Helmholtz Association through its
423 research program ATMO. This represents paper number 21 of the Birmingham Institute of Forest
424 Research.

425 **Author's contribution**

426 The research question to this paper has been developed and proposed by the GGCMCI coordinators
427 J.E. and C.M. J.E. and J.C. performed the post-processing as aggregating the submitted data from grid
428 cell-level to coarser spatial units. C.M. and V.P. conducted the analysis. V.P. wrote the manuscript
429 with substantial contributions from C.M., P.C., D.R., T.I., J.E, D.D., R.C.I, and C.J. All co-authors
430 provided data to the GGCMCI project, discussed, and commented on the manuscript.

431 **References**

- 432 Anderson, W., You, L., Wood, S., Wood-Sichra, U., Wu, W., 2015. An analysis of methodological and
 433 spatial differences in global cropping systems models and maps. *Global Ecol Biogeogr* 24(2), 180-191,
 434 DOI: 10.1111/geb.12243.
- 435 Asseng, S., Ewert, F., Martre, P., Rotter, R.P., Lobell, D.B., Cammarano, D., Kimball, B.A., Ottman, M.J.,
 436 Wall, G.W., White, J.W., Reynolds, M.P., Alderman, P.D., Prasad, P.V.V., Aggarwal, P.K., Anothai, J.,
 437 Basso, B., Biernath, C., Challinor, A.J., De Sanctis, G., Doltra, J., Fereres, E., Garcia-Vila, M., Gayler, S.,
 438 Hoogenboom, G., Hunt, L.A., Izaurrealde, R.C., Jabloun, M., Jones, C.D., Kersebaum, K.C., Koehler, A.K.,
 439 Muller, C., Naresh Kumar, S., Nendel, C., O'Leary, G., Olesen, J.E., Palosuo, T., Priesack, E., Eyshi
 440 Rezaei, E., Ruane, A.C., Semenov, M.A., Shcherbak, I., Stockle, C., Stratonovitch, P., Streck, T., Supit, I.,
 441 Tao, F., Thorburn, P.J., Waha, K., Wang, E., Wallach, D., Wolf, J., Zhao, Z., Zhu, Y., 2015. Rising
 442 temperatures reduce global wheat production. *Nature Clim. Change* 5(2), 143-147, DOI:
 443 10.1038/nclimate2470.
- 444 Balkovič, J., van der Velde, M., Schmid, E., Skalský, R., Khabarov, N., Obersteiner, M., Stürmer, B.,
 445 Xiong, W., 2013. Pan-European crop modelling with EPIC: Implementation, up-scaling and regional
 446 crop yield validation. *Agric. Syst* 120, 61-75, DOI: 10.1016/j.agsy.2013.05.008.
- 447 Batjes, N.H., 2006. ISRIC-WISE derived soil properties on a 5 by 5 arc-minutes global grid (version
 448 1.1). Report 2006/02 (<http://www.isric.org>). SRIC- World Soil Information, Wageningen, Netherlands.
- 449 Becker, R.A., Chambers, J.M., Wilks, A.R., 1988. The new S language: A programming environment
 450 for data analysis and graphics, Wadsworth and Brooks/Cole Advanced Books & Software.USA.
- 451 Bondeau, A., Smith, P.C., Zaehle, S., Schaphoff, S., Lucht, W., Cramer, W., Gerten, D., Lotze-Campen,
 452 H., Müller, C., Reichstein, M., Smith, B., 2007. Modelling the role of agriculture for the 20th century
 453 global terrestrial carbon balance. *Glob Change Biol* 13 (3), 679-706, DOI: 10.1111/j.1365-
 454 2486.2006.01305.x.
- 455 Beddow, J.M., Pardey, P.G., 2015. Moving matters: The effect of location on crop production. *The J.*
 456 *Econ. Hist.* 75(01), 219-249, DOI: doi:10.1017/S002205071500008X.
- 457 Cai, X., Rosegrant, M.W., 2002. Global water demand and supply projections. *Water Int* 27 (2), 159-
 458 169, DOI: 10.1080/02508060208686989.
- 459 Challinor, A.J., Watson, J., Lobell, D.B., Howden, S.M., Smith, D.R., Chhetri, N., 2014. A meta-analysis
 460 of crop yield under climate change and adaptation. *Nature Clim. Change* 4(4), 287-291, DOI:
 461 10.1038/nclimate2153.
- 462 Cosby, B.J., Hornberger, G.M., Clapp, R.B., Ginn, T.R., 1984. A statistical exploration of the
 463 relationships of soil moisture characteristics to the physical properties of soils. *Water Resour. Res* 20
 464 (6), 682-690, DOI: 10.1029/WR020i006p00682.
- 465 de Wit, A.J.W., van Diepen, C.A., 2008. Crop growth modelling and crop yield forecasting using
 466 satellite-derived meteorological inputs. *Int. J. Appl. Earth Obs. Geoinf.* 10(4), 414-425, DOI:
 467 10.1016/j.jag.2007.10.004.
- 468 Deryng, D., Conway, D., Ramankutty, N., Price, J., Warren, R., 2014. Global crop yield response to
 469 extreme heat stress under multiple climate change futures. *Environ. Res. Lett.* 9 (3), 034011, DOI:
 470 10.1088/1748-9326/9/3/034011
- 471 Deryng, D., Sacks, W.J., Barford, C.C., Ramankutty, N., 2011. Simulating the effects of climate and
 472 agricultural management practices on global crop yield. *Global Biogeochem. Cy*, 25 (2), GB2006, DOI:
 473 10.1029/2009GB003765.
- 474 Dietrich, J.P., Schmitz, C., Lotze-Campen, H., Popp, A., Müller, C., 2014. Forecasting technological
 475 change in agriculture—an endogenous implementation in a global land use model. *Technol. Forecast*
 476 *Soc.* 81, 236-249, DOI: doi.org/10.1016/j.techfore.2013.02.003.
- 477 Dobos, E., 2006. Albedo. In *Encyclopedia of Soil Science*, Second Edition., 64-66.
- 478 Drewniak, B., Song, J., Prell, J., Kotamarthi, V.R., Jacob, R., 2013. Modeling agriculture in the
 479 community land model. *Geosci. Model Dev.* 6 (2), 495-515, DOI: 10.5194/gmd-6-495-2013.

480 Eitelberg, D.A., van Vliet, J., Verburg, P.H., 2015. A review of global potentially available cropland
481 estimates and their consequences for model-based assessments. *Glob. Change Biol.* 21 (3), 1236-
482 1248, DOI: 10.1111/gcb.12733.

483 Elliott, J., Kelly, D., Chryssanthacopoulos, J., Glotter, M., Jhunhnuwala, K., Best, N., Wilde, M., Foster,
484 I., 2014. The parallel system for integrating impact models and sectors (PSIMS). *Environ. Model.*
485 *Softw.* 62, 509-516, DOI: 10.1016/j.envsoft.2014.04.008.

486 Elliott, J., Müller, C., Deryng, D., Chryssanthacopoulos, J., Boote, K.J., Büchner, M., Foster, I., Glotter,
487 M., Heinke, J., Iizumi, T., Izaurrealde, R.C., Mueller, N.D., Ray, D.K., Rosenzweig, C., Ruane, A.C.,
488 Sheffield, J., 2015. The global gridded crop model intercomparison: Data and modeling protocols for
489 phase 1 (v1.0). *Geosci. Model Dev.* 8(2), 261-277, DOI: 10.5194/gmd-8-261-2015.

490 FAO, 2014. FAOSTAT: Agricultural production. from: <http://faostat.fao.org/>, date: 2014/09/29.

491 Farquhar, G.D., von Caemmerer, S., Berry, J.A., 1980. A biochemical model of photosynthetic CO₂
492 assimilation in leaves of C₃ species. *Planta* 149 (1), 78-90, DOI: 10.1007/BF00386231.

493 Fila, G., Bellocchi, G., Acutis, M., Donatelli, M., 2003. Irene: A software to evaluate model
494 performance. *Eur. J. Agron.* 18(3), 369-372, DOI: 10.1016/S1161-0301(02)00129-6.

495 Fischer, G., Nachtergaele, F., Prieler, S., Teixeira, E., Tóth, G., van Velthuisen, H., Verelst, L., Wiberg,
496 D., 2012. Global agro-ecological zones (GAEZ v3. 0) - Model documentation. International Institute
497 for Applied Systems Analysis (IIASA), Laxenburg, Austria. Food and Agriculture Organization of the
498 United Nations (FAO) Rome, Italy.

499 Fischer, G., Nachtergaele, F., Prieler, S., van Velthuisen, H.T., Verelst, L., Wiberg, D., 2008. Global
500 agro-ecological zones assessment for agriculture (GAEZ 2008).

501 Fritz, S., See, L., McCallum, I., You, L., Bun, A., Moltchanova, E., Duerauer, M., Albrecht, F., Schill, C.,
502 Perger, C., Havlik, P., Mosnier, A., Thornton, P., Wood-Sichra, U., Herrero, M., Becker-Reshef, I.,
503 Justice, C., Hansen, M., Gong, P., Abdel Aziz, S., Cipriani, A., Cumani, R., Cecchi, G., Conchedda, G.,
504 Ferreira, S., Gomez, A., Haffani, M., Kayitakire, F., Malanding, J., Mueller, R., Newby, T., Nonguierma,
505 A., Olusegun, A., Ortner, S., Rajak, D.R., Rocha, J., Schepaschenko, D., Schepaschenko, M., Terekhov,
506 A., Tiangwa, A., Vancutsem, C., Vintrou, E., Wenbin, W., van der Velde, M., Dunwoody, A., Kraxner, F.,
507 Obersteiner, M., 2015. Mapping global cropland and field size. *Glob. Change Biol.*, DOI:
508 10.1111/gcb.12838.

509 Hall, F.G., Brown de Colstoun, E., Collatz, G.J., Landis, D., Dirmeyer, P., Betts, A., Huffman, G.J.,
510 Bounoua, L., Meeson, B., 2006. Isclsc initiative ii global data sets: Surface boundary conditions and
511 atmospheric forcings for land-atmosphere studies. *J. Geophys. Res. : Atmospheres* 111(D22), D22S01,
512 DOI: 10.1029/2006JD007366.

513 Havlík, P., Schneider, U.A., Schmid, E., Böttcher, H., Fritz, S., Skalský, R., Aoki, K., Cara, S.D.,
514 Kindermann, G., Kraxner, F., Leduc, S., McCallum, I., Mosnier, A., Sauer, T., Obersteiner, M., 2011.
515 Global land-use implications of first and second generation biofuel targets. *Energ. Policy* 39(10),
516 5690-5702, DOI: 10.1016/j.enpol.2010.03.030.

517 Havlík, P., Valin, H., Mosnier, A., Obersteiner, M., Baker, J.S., Herrero, M., Rufino, M.C., Schmid, E.,
518 2012. Crop productivity and the global livestock sector: Implications for land use change and
519 greenhouse gas emissions. *American Journal of Agricultural Economics*, DOI: 10.1093/ajae/aas085.

520 Lotze-Campen, H., Müller, C., Bondeau, A., Rost, S., Popp, A., Lucht, W., 2008. Global food demand,
521 productivity growth, and the scarcity of land and water resources: A spatially explicit mathematical
522 programming approach. *Agr. Econ.* 39(3), 325-338, DOI: 10.1111/j.1574-0862.2008.00336.x.

523 Iizumi, T., Yokozawa, M., Sakurai, G., Travasso, M.I., Romanenkov, V., Oettli, P., Newby, T., Ishigooka,
524 Y., Furuya, J., 2014. Historical changes in global yields: Major cereal and legume crops from 1982 to
525 2006. *Global Ecol. Biogeogr.* 23 (3), 346-357, DOI: 10.1111/geb.12120.

526 Izaurrealde, R.C., McGill, W.B., Williams, J.R., 2012. Chapter 17 - development and application of the
527 epic model for carbon cycle, greenhouse gas mitigation, and biofuel studies. *Managing agricultural*
528 *greenhouse gases.* Liebig, Mark A. , Franzluebbers, Alan J. and Follett, Ronald F. San Diego, Academic
529 Press: 293-308.

530 Izaurrealde, R.C., Williams, J.R., McGill, W.B., Rosenberg, N.J., Jakas, M.C.Q., 2006. Simulating soil c
531 dynamics with epic: Model description and testing against long-term data. *Ecol. Model.* 192 (3–4),
532 362-384, DOI: 10.1016/j.ecolmodel.2005.07.010.

533 Jones, J.W., Hoogenboom, G., Porter, C.H., Boote, K.J., Batchelor, W.D., Hunt, L.A., Wilkens, P.W.,
534 Singh, U., Gijsman, A.J., Ritchie, J.T., 2003. The DSSAT cropping system model. *Eur. J. Agron.* 18(3-4),
535 235-265, DOI: 10.1016/s1161-0301(02)00107-7.

536 Keating, B.A., Carberry, P.S., Hammer, G.L., Probert, M.E., Robertson, M.J., Holzworth, D., Huth, N.I.,
537 Hargreaves, J.N.G., Meinke, H., Hochman, Z., McLean, G., Verburg, K., Snow, V., Dimes, J.P., Silburn,
538 M., Wang, E., Brown, S., Bristow, K.L., Asseng, S., Chapman, S., McCown, R.L., Freebairn, D.M., Smith,
539 C.J., 2003. An overview of APSIM, a model designed for farming systems simulation. *Eur. J. Agron.* 18
540 (3–4), 267-288, DOI: 10.1016/S1161-0301(02)00108-9.

541 Lawrence, D., Slater, A., 2008. Incorporating organic soil into a global climate model. *Clim. Dyn.* 30(2-
542 3), 145-160, DOI: 10.1007/s00382-007-0278-1.

543 Leff, B., Ramankutty, N., Foley, J.A., 2004. Geographic distribution of major crops across the world.
544 *Global Biogeochem. Cy.* 18 (1), DOI: 10.1029/2003GB002108.

545 Lindeskog, M., Arneeth, A., Bondeau, A., Waha, K., Seaquist, J., Olin, S., Smith, B., 2013. Implications
546 of accounting for land use in simulations of ecosystem carbon cycling in africa. *Earth Syst. Dynam.* 4
547 (2), 385-407, DOI: 10.5194/esd-4-385-2013.

548 Liu, J., Williams, J.R., Zehnder, A.J.B., Yang, H., 2007. Gepic - modelling wheat yield and crop water
549 productivity with high resolution on a global scale. *Agric. Syst.* 94 (2), 478-493, DOI:
550 10.1016/j.agry.2006.11.019.

551 Liu, W., Yang, H., Folberth, C., Wang, X., Luo, Q., Schulin, R., 2016. Global investigation of impacts of
552 pet methods on simulating crop-water relations for maize. *Agr. Forest Meteorol.* 221, 164-175, DOI:
553 10.1016/j.agrformet.2016.02.017.

554 Monfreda, C., Ramankutty, N., Foley, J.A., 2008. Farming the planet: 2. Geographic distribution of
555 crop areas, yields, physiological types, and net primary production in the year 2000. *Global*
556 *Biogeochem. Cy.* 22 (1), GB1022, DOI: 10.1029/2007GB002947.

557 Mueller, N.D., Gerber, J.S., Johnston, M., Ray, D.K., Ramankutty, N., Foley, J.A., 2012. Closing yield
558 gaps through nutrient and water management. *Nature* 490 (7419), 254-257, DOI:
559 10.1038/nature11420.

560 Müller, C., Elliott, J., Chryssanthacopoulos, J., Deryng, D., Folberth, C., Pugh, T.A.M., Schmid, E., 2015.
561 Implications of climate mitigation for future agricultural production. *Environ. Res. Lett.* 10(12),
562 125004, DOI: 10.1088/1748-9326/10/12/125004.

563 Müller, C., Robertson, R.D., 2014. Projecting future crop productivity for global economic modeling.
564 *Agr. Econ.* 45 (1), 37-50, DOI: 10.1111/agec.12088.

565 Nelson, G.C., Valin, H., Sands, R.D., Havlík, P., Ahammad, H., Deryng, D., Elliott, J., Fujimori, S.,
566 Hasegawa, T., Heyhoe, E., Kyle, P., Von Lampe, M., Lotze-Campen, H., Mason d’Croz, D., van Meijl, H.,
567 van der Mensbrugge, D., Müller, C., Popp, A., Robertson, R., Robinson, S., Schmid, E., Schmitz, C.,
568 Tabeau, A., Willenbockel, D., 2014a. Climate change effects on agriculture: Economic responses to
569 biophysical shocks. *Proc. Natl. Acad. Sci. USA* 111(9), 3274-3279, DOI: 10.1073/pnas.1222465110.

570 Nelson, G.C., van der Mensbrugge, D., Ahammad, H., Blanc, E., Calvin, K., Hasegawa, T., Havlik, P.,
571 Heyhoe, E., Kyle, P., Lotze-Campen, H., von Lampe, M., Mason d’Croz, D., van Meijl, H., Müller, C.,
572 Reilly, J., Robertson, R., Sands, R.D., Schmitz, C., Tabeau, A., Takahashi, K., Valin, H., Willenbockel, D.,
573 2014b. Agriculture and climate change in global scenarios: Why don't the models agree. *Agr. Econ.* 45
574 (1), 85-101, DOI: 10.1111/agec.12091.

575 Osborne, T., Rose, G., Wheeler, T., 2013. Variation in the global-scale impacts of climate change on
576 crop productivity due to climate model uncertainty and adaptation. *Agr. Forest Meteorol.* 170, 183-
577 194, DOI: 10.1016/j.agrformet.2012.07.006.

578 Portmann, F.T., Siebert, S., Döll, P., 2010. Mirca2000—global monthly irrigated and rainfed crop
579 areas around the year 2000: A new high-resolution data set for agricultural and hydrological
580 modeling. *Global Biogeochem. Cy.* 24 (1), GB1011, DOI: 10.1029/2008GB003435.

581 Pugh, T.A.M., Arneth, A., Olin, S., Ahlström, A., Bayer, A.D., Goldewijk, K.K., Lindeskog, M., Schurgers,
582 G., 2015. Simulated carbon emissions from land-use change are substantially enhanced by
583 accounting for agricultural management. *Environ. Res. Lett.* 10(12), DOI: 10.1088/1748-
584 9326/10/12/124008

585 R Development Core Team (2014). R: A language and environment for statistical computing.
586 Computing, R Foundation for Statistical. Vienna, Austria.

587 Ramankutty, N., Evan, A.T., Monfreda, C., Foley, J.A., 2008. Farming the planet: 1. Geographic
588 distribution of global agricultural lands in the year 2000. *Global Biogeochem. Cy.* 22 (1), GB1003, DOI:
589 10.1029/2007GB002952.

590 Ray, D.K., Ramankutty, N., Mueller, N.D., West, P.C., Foley, J.A., 2012. Recent patterns of crop yield
591 growth and stagnation. *Nat. Commun.* 3, DOI: 10.1038/ncomms2296.

592 Rosenzweig, C., Elliott, J., Deryng, D., Ruane, A.C., Müller, C., Arneth, A., Boote, K.J., Folberth, C.,
593 Glotter, M., Khabarov, N., Neumann, K., Piontek, F., Pugh, T.A.M., Schmid, E., Stehfest, E., Yang, H.,
594 Jones, J.W., 2014. Assessing agricultural risks of climate change in the 21st century in a global gridded
595 crop model intercomparison. *Proc. Natl. Acad. Sci. U.S.A.* 111 (9), 3268-3273, DOI:
596 10.1073/pnas.1222463110.

597 Rosenzweig, C., Jones, J.W., Hatfield, J.L., Ruane, A.C., Boote, K.J., Thorburn, P., Antle, J.M., Nelson,
598 G.C., Porter, C., Janssen, S., Asseng, S., Basso, B., Ewert, F., Wallach, D., Baigorria, G., Winter, J.M.,
599 2013. The agricultural model intercomparison and improvement project (AgMIP): Protocols and pilot
600 studies. *Agr. and Forest Meteorol.* 170, 166-182, DOI: 10.1016/j.agrformet.2012.09.011.

601 Rötter, R.P., Palosuo, T., Kersebaum, K.C., Angulo, C., Bindi, M., Ewert, F., Ferrise, R., Hlavinka, P.,
602 Moriondo, M., Nendel, C., Olesen, J.E., Patil, R.H., Ruget, F., Taká, J., Trnka, M., 2012. Simulation of
603 spring barley yield in different climatic zones of northern and central Europe: A comparison of nine
604 crop models. *Field Crop. Res.* 133, 23-36, DOI: 10.1016/j.fcr.2012.03.016.

605 Roux, S., Brun, F., Wallach, D., 2014. Combining input uncertainty and residual error in crop model
606 predictions: A case study on vineyards. *Eur. J. Agron.* 52 (Part B), 191-197,
607 DOI:10.1016/j.eja.2013.09.008.

608 Ruane, A.C., Goldberg, R., Chryssanthacopoulos, J., 2015. Climate forcing datasets for agricultural
609 modeling: Merged products for gap-filling and historical climate series estimation. *Agr. and Forest*
610 *Meteorol.* 200, 233-248, DOI: 10.1016/j.agrformet.2014.09.016.

611 Sacks, W.J., Deryng, D., Foley, J.A., Ramankutty, N., 2010. Crop planting dates: An analysis of global
612 patterns. *Global Ecol. Biogeogr.* 19 (5), 607-620, DOI: 10.1111/j.1466-8238.2010.00551.x.

613 Sakurai, G., Iizumi, T., Nishimori, M., Yokozawa, M., 2014. How much has the increase in atmospheric
614 CO₂ directly affected past soybean production? *Scientific Reports* 4, 4978, DOI: 10.1038/srep04978.

615 Schaap, M.G., Bouten, W., 1996. Modeling water retention curves of sandy soils using neural
616 networks. *Water Resour. Res.* 32 (10), 3033-3040, DOI: 10.1029/96WR02278.

617 Schmitz, C., van Meijl, H., Kyle, P., Nelson, G.C., Fujimori, S., Gurgel, A., Havlik, P., Heyhoe, E., d'Croz,
618 D.M., Popp, A., Sands, R., Tabeau, A., van der Mensbrugghe, D., von Lampe, M., Wise, M., Blanc, E.,
619 Hasegawa, T., Kavallari, A., Valin, H., 2014. Land-use change trajectories up to 2050: Insights from a
620 global agro-economic model comparison. *Agr. Econ.* 45 (1), 69-84, DOI: 10.1111/agec.12090.

621 See, L., Fritz, S., You, L., Ramankutty, N., Herrero, M., Justice, C., Becker-Reshef, I., Thornton, P., Erb,
622 K., Gong, P., Tang, H., van der Velde, M., Ericksen, P., McCallum, I., Kraxner, F., Obersteiner, M., 2015.
623 Improved global cropland data as an essential ingredient for food security. *Glob. Food Sec.* 4, 37-45,
624 DOI: 10.1016/j.gfs.2014.10.004.

625 Siebert, S., Döll, P., Feick, S., Frenken, K., Hoogeveen, J., 2007. Global map of irrigation areas version
626 4.0.1. University of Frankfurt (Main), Germany, and FAO, Rome, Italy.

627 Siebert, S., Döll, P., Hoogeveen, J., Faures, J.M., Frenken, K., Feick, S., 2005. Development and
628 validation of the global map of irrigation areas. *Hydrol. Earth Syst. Sci.* 9 (5), 535-547, DOI:
629 10.5194/hess-9-535-2005.

630 Smith, B., Prentice, I.C., Sykes, M.T., 2001. Representation of vegetation dynamics in the modelling of
631 terrestrial ecosystems: Comparing two contrasting approaches within European climate space.
632 *Global Ecol. Biogeogr.* 10 (6), 621-637, DOI: 10.1046/j.1466-822X.2001.t01-1-00256.x.

633 Thoning, K.W., Tans, P.P., Komhyr, W.D., 1989. Atmospheric carbon dioxide at Mauna Loa
634 observatory: 2. Analysis of the NOAA GMCC data, 1974–1985. *J. Geophys. Res. : Atmospheres* 94
635 (D6), 8549-8565, DOI: 10.1029/JD094iD06p08549.

636 USDA,NRCS, 2015. Web soil survey. from: <http://websoilsurvey.nrcs.usda.gov/> (accessed:
637 09.11.2015).

638 Van Genuchten, M.T., Leij, F., Lund, L. 1992. Indirect methods for estimating the hydraulic properties
639 of unsaturated soils, University of California, Riverside, USA.

640 van Wart, J., van Bussel, L.G.J., Wolf, J., Licker, R., Grassini, P., Nelson, A., Boogaard, H., Gerber, J.,
641 Mueller, N.D., Claessens, L., van Ittersum, M.K., Cassman, K.G., 2013. Use of agro-climatic zones to
642 upscale simulated crop yield potential. *Field Crop. Res.* 143, 44-55, DOI: 10.1016/j.fcr.2012.11.023.

643 Waha, K., van Bussel, L.G.J., Müller, C., Bondeau, A., 2012. Climate-driven simulation of global crop
644 sowing dates. *Global Ecol. Biogeogr.* 21 (2), 247-259, DOI: 10.1111/j.1466-8238.2011.00678.x.

645 Wheeler, T., von Braun, J., 2013. Climate change impacts on global food security. *Science* 341(6145),
646 508-513, DOI: 10.1126/science.1239402.

647 Williams, J.R., 1995. The EPIC model. *Computer models of watershed hydrology*. Littleton, CO: 909-
648 1000.

649 Willmott, C., Ackleson, S., Davis, R., Feddema, J., Klink, K., Legates, D., O'Donnell, J., Rowe, C., 1985.
650 Statistics for the evaluation and comparison of models. *J. Geophys. Res.* 90 (C5), 8995-9005, DOI:
651 10.1029/JC090iC05p08995.

652 Wu, X., Vuichard, N., Ciais, P., Viovy, N., de Noblet-Ducoudré, N., Wang, X., Magliulo, V., Wattenbach,
653 M., Vitale, L., Di Tommasi, P., Moors, E.J., Jans, W., Elbers, J., Ceschia, E., Tallec, T., Bernhofer, C.,
654 Grünwald, T., Moureaux, C., Manise, T., Ligne, A., Cellier, P., Loubet, B., Larmanou, E., Ripoche, D.,
655 2015. Orchidee-crop (v0), a new process based agro-land surface model: Model description and
656 evaluation over Europe. *Geosci. Model Dev. Discuss.* 8 (6), 4653-4696, DOI: 10.5194/gmdd-8-4653-
657 2015.

658 You, L., Wood, S., Wood-Sichra, U., Wu, W., 2014. Generating global crop distribution maps: From
659 census to grid. *Agric. Syst* 127, 53-60, DOI: 10.1016/j.agry.2014.01.002.

660

Figure

[Click here to download Figure: Fig.1.docx](#)

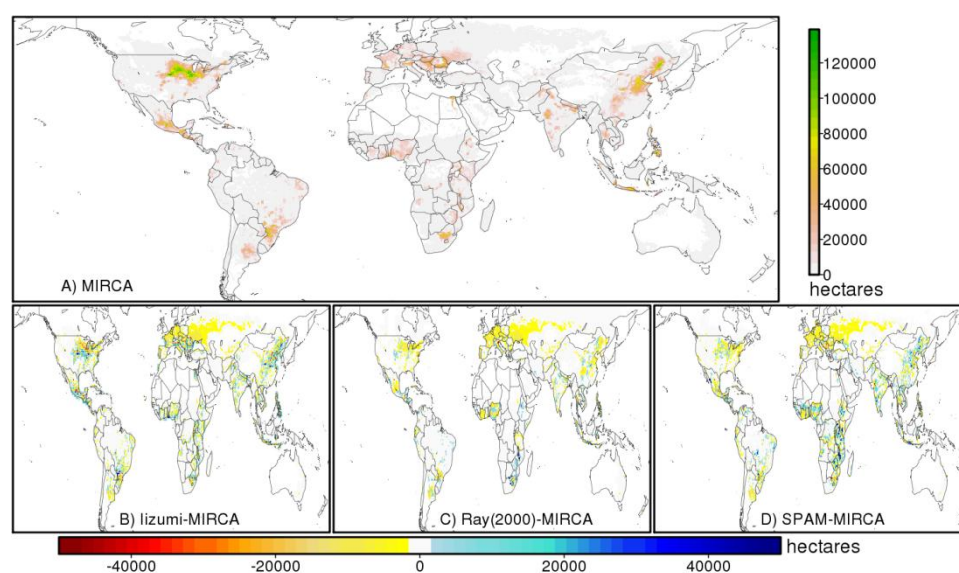


Fig. 1: Maps of spatial patterns of total harvested maize area according to MIRCA2000 (panel A) and the absolute differences in ha over 0.5° grid cells between IZUMI (panel B), Ray (time slice for the year 2000 in panel C), and SPAM2005 (panel D) and MIRCA2000 respectively. See the same figure for irrigated areas only in *SI Appendix, Fig. B.1*.

Figure

[Click here to download Figure: Fig.2.docx](#)

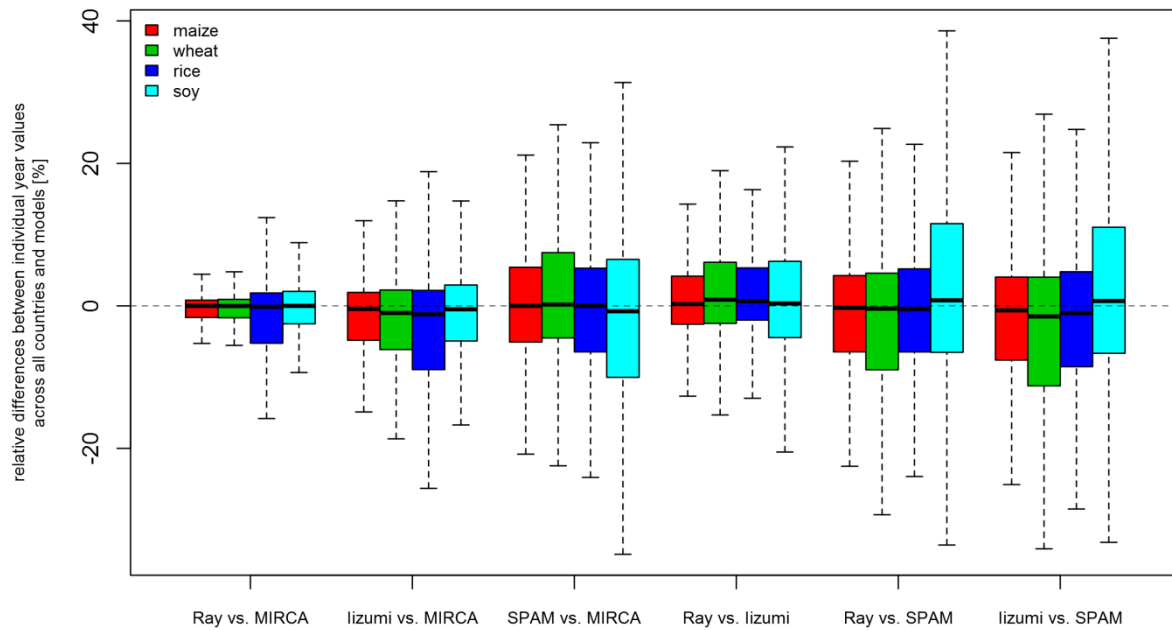


Fig.2: Boxplots of relative differences (%) between aggregated yield time series (t/ha) over 208 countries, 14 GCMs and 31 years of the weather data set AgMERRA for the four crop types (n= 357365 for maize, n= 290061 for wheat, n= 214617 for rice, n= 202619 for soybean). Boxes show the interquartile (25-75%) range across the GCMs used, whiskers expand to 1.5 times of inner-quartile range of national aggregated yield, and black lines within the boxes display the median value (outliers are not displayed).

Figure

[Click here to download Figure: Fig.3.docx](#)

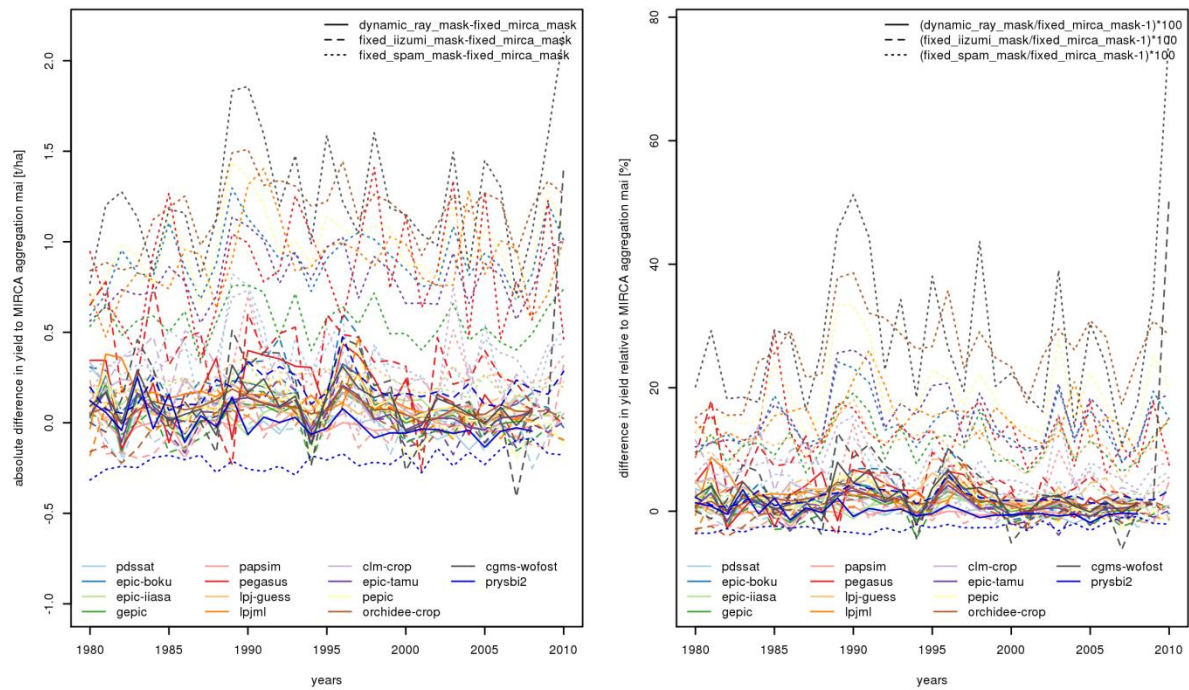


Fig. 3: Absolute (t/ha) (left panel) and (right panel) relative difference (%) between nationally annual aggregated yield time series displayed for the example case of maize yield (DM t/ha) in France. Difference per model, year, and mask from the four aggregation sets is largest with the SPAM aggregation (dotted lines) and for most models accounting for about one additional t/ha.

Figure

[Click here to download Figure: Fig.4.docx](#)

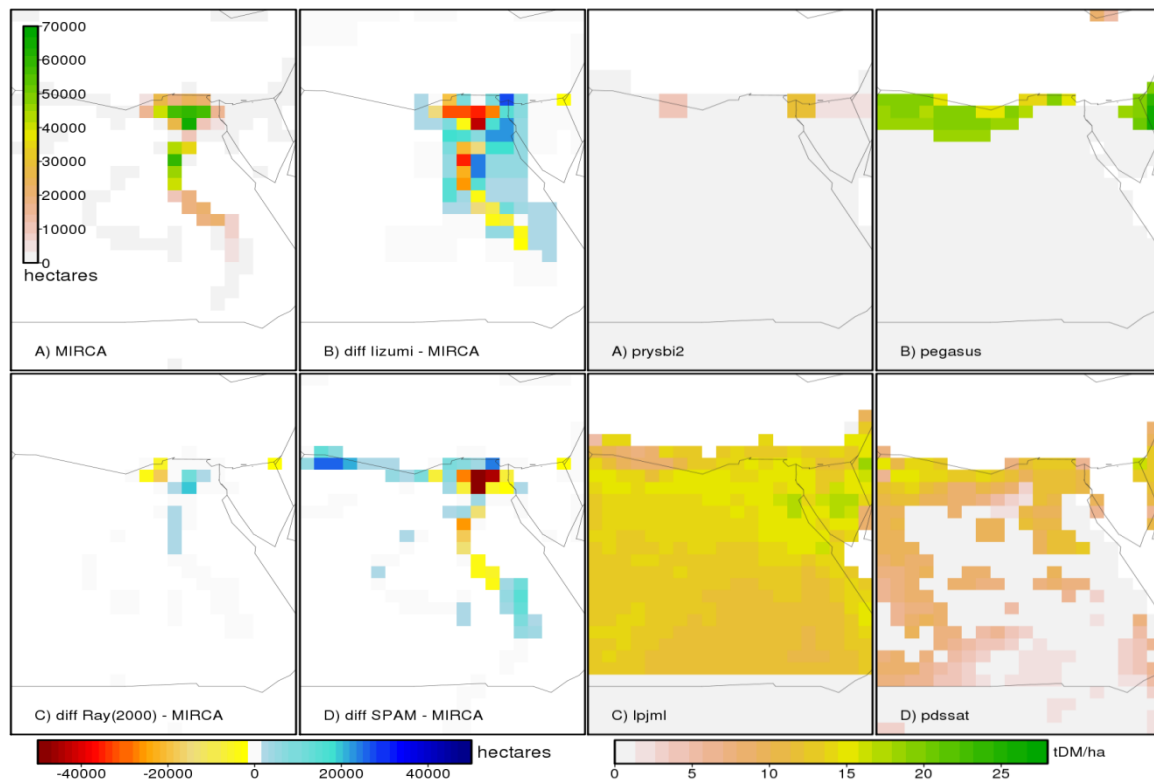


Fig. 4: (Left panel) For irrigated maize harvested areas (ha) in Egypt, spatial patterns and quantities differ between the crop masks. The maps show grid cell scale harvested area as reported by MIRCA2000 (A), and the absolute differences between harvested areas of lizumi (B), Ray (C), and SPAM2005 (D) and MIRCA2000, respectively. (Right panel) Spatial patterns of simulated irrigated maize yields, as means over the AgMERRA weather data time period and before any masking by crop-specific harvested area data, supplied by four models A) PRYSBI2, B) PEGASUS, C) LPJmL, and D) pDSSAT. The gray shaded areas indicate grid cells where the climate conditions were regarded as unsuitable to grow irrigated maize by a model.

Figure

[Click here to download Figure: Fig.5.docx](#)

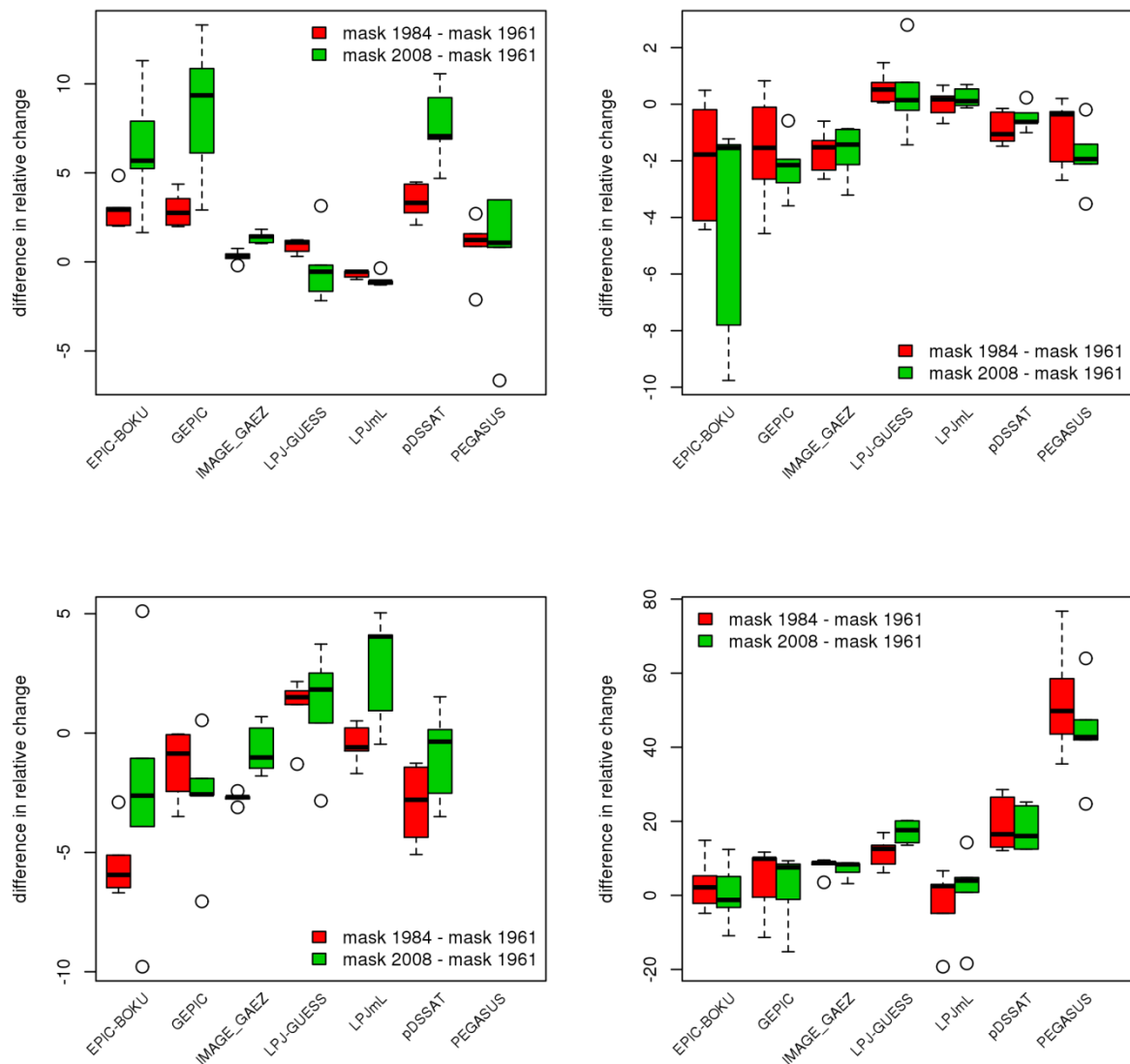


Fig. 5: Differences in projected relative yield changes (percentage change of the period 2070-2099 relative to 1980-2009) between the aggregation with the Ray crop mask of 1961, and that of 1984 (red) and 2008 (green). The panels display aggregated yields for one of the top-10 producer countries for each of the four crops: (Upper left panel) India for maize, (upper right panel) Australia for wheat, (bottom left panel) Brazil for rice, and (bottom right panel) Argentina for soybean. Boxes show the interquartile (25-75%) range across the five GCMs used, whiskers expand to 1.5 times the inner-quartile range of national aggregated yield and outliers are depicted as dots. Black lines within the boxes display the median value.

Supplementary material for on-line publication only

[Click here to download Supplementary material for on-line publication only: SI_index.docx](#)

Supplementary material for on-line publication only

[Click here to download Supplementary material for on-line publication only: SI_A_Details on crop models.docx](#)

Supplementary material for on-line publication only

[Click here to download Supplementary material for on-line publication only: SI_B_Global crop specific harvested area maps.doc](#)

Supplementary material for on-line publication only

[Click here to download Supplementary material for on-line publication only: SI_C_Relative difference between data sets of total](#)

Supplementary material for on-line publication only

[Click here to download Supplementary material for on-line publication only: SI_D_G_Yield_production_harvestedarea.xlsx](#)

Supplementary material for on-line publication only

[Click here to download Supplementary material for on-line publication only: SI_E_Egypt case_graph_time_series_per_model.do](#)

Supplementary material for on-line publication only

[Click here to download Supplementary material for on-line publication only: SI_F_Aggregation of grid cell yield to FPU and coun](#)

Supplementary material for on-line publication only

[Click here to download Supplementary material for on-line publication only: SI_References supplementary information.docx](#)